

Original Article

Efficacy of Single Energy Metal Artifact Reduction (SEMAR) for Head and Neck Cancer

Takumi Oshima, Junichi Tsuchiya and Ukihide Tateishi

Department of Diagnostic Radiology and Nuclear Medicine, Tokyo Medical and Dental University Graduate School of Medical and Dental Sciences, 1-5-45 Yushima Bunkyo-ku, Tokyo 113-8519, Japan

Abstract

Positron-emission tomography/computed tomography (PET/CT) in the head and neck region is susceptible to artifacts caused by dental restorations. Metal artifact reduction is an established technology that can be used to improve the quality of CT images. The diagnostic efficacy of single-energy metal artifact reduction (SEMAR) for head and neck cancer has not been proven. We aimed to investigate the efficacy of SEMAR with PET/CT in the field of head and neck cancer. The study included 46 patients who underwent PET/CT with SEMAR. For qualitative evaluation, images with and without SEMAR were visually evaluated by two radiologists using a 5-point scale. For quantitative assessment, the standardized uptake values (SUVs) -related parameters were assessed based on their position in normal structures such as the tongue, tonsils, masseter muscles, and spinal cord. The qualitative analysis revealed that SEMAR improved the overall quality of PET/CT fusion images (2.28 ± 1.24 points vs. 3.61 ± 0.77 points, $p < 0.0001$). The scores for normal structures were also enhanced. SEMAR did not change the SUV-related values significantly. In conclusion, SEMAR significantly improved the quality of PET/CT fusion images. Thus, SEMAR with PET/CT clearly has potential diagnostic efficacy.

Keywords: Positron-emission tomography/computed tomography, artifact, head and neck neoplasms

Introduction

¹⁸F-fluorodeoxyglucose (FDG) positron-emission tomography (PET) is a functional imaging modality that has an established role in the diagnosis and staging of malignant tumors¹. However, PET images are noisy and low-resolution, which makes them difficult to interpret². The combination of PET and CT is vital when locating the anatomical position of neoplasms and when distinguishing between the uptake of tumors and normal physiology³. CT is also used for attenuation-correction of PET; hybrid PET/CT improves the interpretation of malignant tumors, including head and neck cancer^{2, 4-6}.

Artifacts arising from dental metals impair image quality, which is an obstacle when detecting and analyzing lesions. Various methods are used to reduce artifacts; metal artifact reduction (MAR) is a major technology in CT and its effectiveness has been demonstrated in the head and neck region as well as the chest⁷⁻⁹. Single-energy metal artifact reduction (SEMAR) is a commercially available MAR algorithm that can be applied to single-energy CT; it has been shown to improve image quality and lesion detection within the oral cavity^{10, 11}.

For PET, MAR can improve the image quality in either of two ways: by improving the CT image quality or through attenuation-correction. The higher quality μ -map acquired using CT with MAR can produce more precise PET images¹²⁻¹⁴. Although SEMAR is widely used in the field of CT, the application of SEMAR to PET/CT is not yet to gain widespread popularity. However, the effectiveness of SEMAR in hybrid PET/CT imaging has not been fully demonstrated.

Corresponding Author: Takumi Oshima, M.D.
Department of Diagnostic Radiology and Nuclear Medicine, Tokyo Medical and Dental University Graduate School of Medical and Dental Sciences, 1-5-45 Yushima Bunkyo-ku, Tokyo 113-8519, Japan
Tel: +81-3-3813-6111 Fax: +81-3-3813-6111
E-mail: osmdrnm@tmd.ac.jp
Received July 25; Accepted September 19, 2019

This study was conducted to investigate the effect of SEMAR in PET/CT for head and neck cancer with respect to the image quality and standardized uptake value (SUV)-related parameters.

Materials and Methods

Subjects/Patients

Our study included 46 consecutive patients with suspected head and neck cancer or its recurrence that underwent 18F-FDG-PET/CT at our university hospital between July 2017 and October 2017. Patients who were less than 20 years old, patients who were pregnant or breastfeeding, and patients whose blood sugar levels exceeded 200 mg/dl at the time of the scan were excluded. Informed consent was obtained for each patient. This study was certified by the Ethics Committee in the Tokyo Medical and Dental University (certification number: M2019-074).

Data acquisition

Examinations were performed using a PET/CT (Celerion™, Canon Medical Systems, Tokyo, Japan) at our university. CT data were acquired with 120 kVp, 40 mA, 0.938 of pitch factor, and 1.0 s of rotation time. PET data were acquired with 1 bed 240 s and a 3 mm Gaussian filter, then reconstructed with time-of-flight three-dimensional ordered subset expectation maximization (TOF 3D OSEM). For each scan, PET/CT fusion images with and without SEMAR were produced.

Qualitative evaluation

For evaluation, 512×512 pixel images with a slice thickness of 5.0 mm were produced. To evaluate the CT images, the window width and window level of the CT were fixed at 350 and 40, respectively. The field of view was set to 16 cm.

Two radiologists, with two and eight years of experience, evaluated the images. From the PET/CT fusion images, an axial image that included the tongue, tonsils, masseter muscles, and spinal cord was selected by an evaluator. The image quality of non-SEMAR and SEMAR images of the chosen slice were visually graded by the two radiologists using a five-point scheme: from 1 (poor) to 5 (excellent). In addition to the overall evaluation, we also graded normal constructions in the same axial image, including the tongue, tonsil, masseter muscles, and spinal cord. For each patient, the non-SEMAR and SEMAR images were graded individually.

Quantitative evaluation

For each patient scan, axial images with or without SEMAR at the level of teeth were selected by an evaluator. On each axial image, regions of interest (ROIs)¹⁵ with a diameter of 10 mm were manually positioned for the tongue, tonsil, masseter muscle, and spinal cord. For the tonsil and the masseter muscle, either the right or left organ was chosen for the measurement. The ROIs were placed on the center of each organ to measure uptake accuracy. For each ROI, the mean standardized uptake value (SUV_{mean}), maximum standardized uptake value¹⁶, metabolic tumor volume (MTV), and total lesion glycolysis (TLG) were measured. The standard deviations (SDs) of SUV were also calculated in order to evaluate the noise.

Statistical analysis

In the qualitative evaluation, a paired Wilcoxon signed-rank test was used to illustrate the difference between the scores of the SEMAR and non-SEMAR images. The inter-observer agreements were calculated for all 460 scores using a weighted Kappa test. In the quantitative evaluation, Student's paired t-test was used to compare the data.¹⁷

Results

In total, 46 patients (27 males and 19 females; mean age: 65.5 years, age range: 34–91 years) were included in the study. Ten patients underwent PET/CT for the staging of head and neck cancer, while the remaining 36 patients underwent the procedure to detect its recurrence. Among the patients, 40 had one or more dental restorations visible in the image, whereas six had no metallic density in the head and neck region. Patient characteristics are shown in Table 1.

Representative images with and without SEMAR are shown in Fig. 1. The overall score for the SEMAR images (3.6 ± 0.8) was significantly higher than that for the non-SEMAR images (2.3 ± 1.2) (Table 2). The score improved with SEMAR by 1 point in 15 cases, 2 points in 20 cases, and more than 3 points in 2 cases. In 9 cases, the score did not improve or worsened by 1 point. The scores for the normal structures, including the tongue, tonsil, masseter muscle, and spinal cord, were also significantly improved using SEMAR (Table 2). Among the normal structures, the scores for the spinal cord were highest, followed by the tonsil, masseter muscle, and tongue in descending order. In most cases SEMAR improved the quality of the images. However, the image quality degraded in four of the 46 patients (8%). One of the four cases is shown in Fig. 2. In the qualitative evaluation, substantial

Table 1. Summary of patient characteristics

Sex		
Male/Female	27/19	
Age (years)	65.5 ± 13.3	(34-91)
Indication for PET/CT		
Staging/Detection of disease	10	
Detection of recurrence	36	
Dental Implants		
None/unilateral/bilateral	6/20/20	
Types of Cancer		
Lingual	22	
Others*	24	

Age is given in means ± standard deviation (range)

*Others include cancer of the gingiva, floor of mouth, buccal mucosa, soft palate, and retromolar triangle.

Table 2. Qualitative evaluation of non-SEMAR and SEMAR PET/CT images

	non-SEMAR	SEMAR	
Overall	2.3 ± 1.2	3.6 ± 0.8	*
Tongue	2.0 ± 1.4	3.3 ± 1.0	*
Tonsils	3.1 ± 1.1	4.0 ± 0.7	*
Masseter muscles	2.3 ± 1.4	3.5 ± 1.0	*
Spinal cord	3.7 ± 0.8	4.3 ± 0.6	*

n = 46

All data are given as the mean ± standard deviation

SEMAR = single-energy metal artifact reduction

* p<0.01

A paired Wilcoxon signed rank test was used to compare the scores

agreement was shown in the evaluation scores between the two observers (weighted Kappa = 0.79, p < 0.0001).

Virtually all the SUV parameters in the SEMAR and non-SEMAR images did not differ significantly, except for the SUV_{MAX} of the spinal cord, which was slightly higher in the SEMAR images compared to the non-SEMAR images (Table 3). The SD of the SUV in the SEMAR and non-SEMAR images were not significantly different (Table 4).

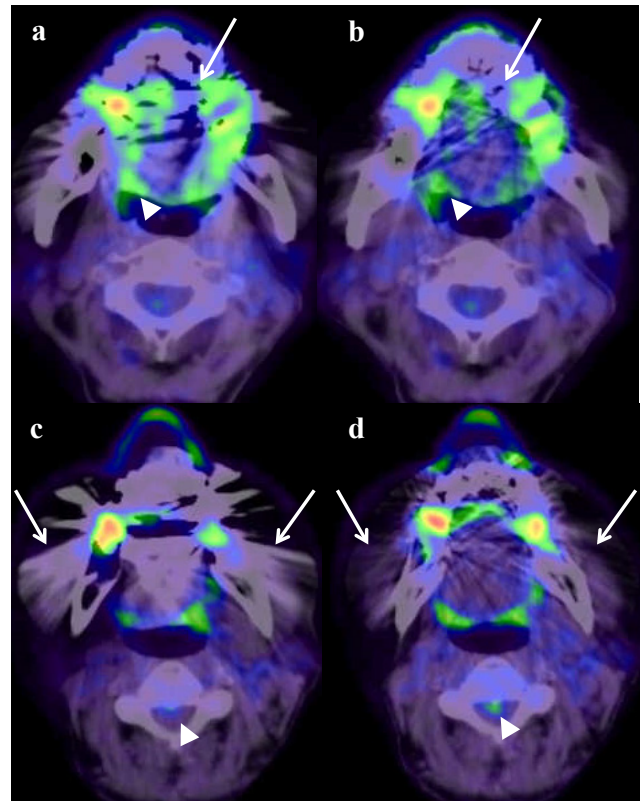


Figure 1. PET/CT fusion images

A 72-year-old man with carcinoma of the gingiva. In the non-SEMAR image (a) both dark and white band artifacts are visible. However, in the SEMAR image (b) the artifacts are reduced inside the oral cavity (arrow) and the spinal canal. With reduction of artifacts in CT, the physiological uptake of the tonsils is better seen in the SEMAR than the non-SEMAR image (arrowhead). A 62-year-old woman with carcinoma of the soft palate. The bilateral masseter muscles (arrow) are not as clear in the non-SEMAR image (c) as they are in the SEMAR image. The physiological uptake of the spinal cord is also clear in the SEMAR image compared to the non-SEMAR image (arrowhead).

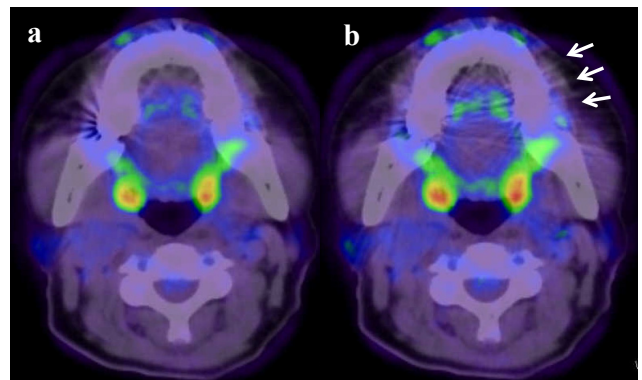


Figure 2. PET/CT fusion images

A 56-year-old woman with carcinoma of the tongue. In the non-SEMAR image, slight streak artifacts are visible (e). In the SEMAR image, (f) the artifacts have significantly increased (arrows).

Table 3. Values of SUV characteristics in non-SEMAR and SEMAR images

SUVmean			
	non-SEMAR	SEMAR	
Tongue	1.63 ± 1.19	1.61 ± 0.98	n.s.
Tonsils	2.18 ± 0.64	2.20 ± 0.67	n.s.
Masseter muscles	0.67 ± 0.17	0.69 ± 0.21	n.s.
Spinal cord	1.38 ± 0.23	1.36 ± 0.16	n.s.
SUVMAX			
	non-SEMAR	SEMAR	
Tongue	1.61 ± 0.98	2.92 ± 1.90	n.s.
Tonsils	4.71 ± 1.65	4.66 ± 1.70	n.s.
Masseter muscles	1.41 ± 0.87	1.43 ± 0.91	n.s.
Spinal cord	2.20 ± 0.43	2.28 ± 0.34	*
Metabolic tumor volume			
	non-SEMAR	SEMAR	
Tongue	2.45 ± 1.05	2.41 ± 1.05	n.s.
Tonsils	1.80 ± 0.71	1.72 ± 0.65	n.s.
Masseter muscles	2.89 ± 0.75	2.89 ± 0.93	n.s.
Spinal cord	2.92 ± 0.70	2.96 ± 0.64	n.s.
Total lesion glycolysis			
	non-SEMAR	SEMAR	
Tongue	4.13 ± 4.36	3.95 ± 3.36	n.s.
Tonsils	3.85 ± 1.98	3.67 ± 1.98	n.s.
Masseter muscles	1.97 ± 0.74	2.05 ± 0.91	n.s.
Spinal cord	4.05 ± 1.22	4.02 ± 1.04	n.s.

n = 46

All data are given as the mean ± standard deviation

SUV = standardized uptake value

* p < 0.05

A paired t-test was used to compare the data

Table 4. Values of the standard deviations of SUV in non-SEMAR and SEMAR images

	non-SEMAR	SEMAR	
Tongue	0.42 ± 0.32	0.48 ± 0.45	n.s.
Tonsils	0.86 ± 0.39	0.86 ± 0.41	n.s.
Masseter muscles	0.21 ± 0.15	0.23 ± 0.18	n.s.
Spinal cord	0.32 ± 0.08	0.32 ± 0.08	n.s.

n = 46

All data are given as the mean ± standard deviation

SEMAR = single-energy metal artifact reduction

A paired t-test was used to compare the data

Discussion

In this study, SEMAR improved the quality of FDG-PET/CT images in the head and neck region, although the SUV-related parameters did not change significantly. Thus, SEMAR may be beneficial for hybrid PET/CT images of the head and neck region, where the complex anatomy must be carefully analyzed.

SEMAR is a type of MAR algorithm; it applies iterative reconstruction (IR) and can be classified into iterative and metal implanting methods¹⁹. It generates artifact-reduced images by eliminating metal artifacts. Unlike dual-energy scanning, the SEMAR algorithm is an IR algorithm based on raw data and it can be applied to single-energy CT after scanning. Previous studies have shown that SEMAR can visually improve the CT images of patients with hip prostheses, metallic embolization coils, and dental prostheses^{8, 10, 19}. In this study, fusion PET/CT images were significantly improved with SEMAR. MAR improves CT images, thus the quality of the PET images is enhanced as the attenuation-correction of PET depends on μ -maps created by CT^{20, 21}. With regard to PET/CT imaging, the dual-energy technique is not applicable to commercially available PET/CT. Moreover, SEMAR is advantageous because it does not require any additional radiation exposure.

In four cases, SEMAR caused contradictory degradation of the image quality. In previous studies, no definite image degradation was described as a result of SEMAR. One study reported that SEMAR sufficiently reduced the artifacts in patients with unilateral dental prostheses but did little to decrease the artifacts in some patients with bilateral dental prostheses, embolization coils, and hip prostheses⁸. Of the four patients, three had a unilateral dental implant and one had no dental implant. The actual cause is not known, but it is possible that the position of the dental restorations affects the use of SEMAR.

Previous reports have also suggested that MAR on PET/CT images may change the SUV parameters depending on the type of artifact^{14, 22}. In a phantom study, over- and under-estimation of the FDG uptake, caused by dark and white streak artifacts respectively, was reduced by correcting the μ -map²¹. In this study, SEMAR had no significant effect on the SUV-related characteristics. This may be because we placed the ROIs without distinguishing between dark and white streak artifacts, such that the artifacts cancelled out. If we had placed the ROIs on small lesions affected by just one type of artifact, we would have obtained more precise SUV parameters. Moreover, Sonoda et al. reported that metallic artifacts were not significantly reduced at distances of

0.5–1.0 cm away from dental restorations⁹. The distance from the dental prostheses could affect the SUV-related parameters, which should be assessed in further studies.

We used various parameters to evaluate changes of data in the PET in this study. Although these parameters are widely used in the field of PET²³, it is difficult to determine which is the most useful in the evaluation of SEMAR images. Further study is required to ascertain which parameters are the most important.

Our study had a few limitations. Firstly, we did not include normal controls and we also excluded obvious tumors when they were visible in the view. However, tumor extension may have affected FDG uptake in the region adjacent to the tumor. Moreover, improved image quality is expected to make the detection of tumors and the assessment of tumor extensions easier, which should be evaluated in further study. Secondly, the sample size was relatively small; consequently, the validity of the result should be assessed in future studies. Finally, we did not blind the observers to whether they were looking at SEMAR or non-SEMAR images, leading to possible bias.

Conclusion

SEMAR improved the quality of the PET/CT fusion images of patients with highly attenuating objects, such as dental restorations, by reducing the artifacts and increasing the precise anatomic delineation of normal structures in the head and neck. SEMAR may thus have a positive impact on PET/CT in the head and neck, which may improve the detectability of cancer or its recurrence, especially in regions adjacent to metallic objects.

Conflict of interest

There are no conflicts of interest to disclose.

Acknowledgement

The authors wish to acknowledge Ms. Masako Akiyama, URA, Research Administration Division, Tokyo Medical and Dental University, for her help in interpreting the significance of the results of this study.

References

- Gambhir SS, Czernin J, Schwimmer J, et al. A tabulated summary of the FDG PET literature. *J Nucl Med.* 2001; 42(5 Suppl):1S-93S.
- Fukui MB, Blodgett TM, Meltzer CC. PET/CT imaging in recurrent head and neck cancer. *Seminars in ultrasound, CT, and MR.* 2003; 24(3):157-63.
- Beyer T, Townsend DW, Brun T, et al. A combined PET/CT scanner for clinical oncology. *J Nucl Med.* 2000; 41(8):1369-79.
- Bar-Shalom R, Guralnik L, Tsalic M, et al. The additional value of PET/CT over PET in FDG imaging of oesophageal cancer. *Eur J Nucl Med Mol Imaging.* 2005; 32(8):918-24.
- Antoch G, Saoudi N, Kuehl H, et al. Accuracy of whole-body dual-modality fluorine-18-2-fluoro-2-deoxy-D-glucose positron emission tomography and computed tomography (FDG-PET/CT) for tumor staging in solid tumors: Comparison with CT and PET. *J Clin Oncol.* 2004; 22(21):4357-68.
- Bar-Shalom R, Yefremov N, Guralnik L, et al. Clinical performance of PET/CT in evaluation of cancer: Additional value for diagnostic imaging and patient management. *J Nucl Med.* 2003; 44(8):1200-9.
- Katsura M, Sato J, Akahane M, et al. Current and novel techniques for metal artifact reduction at CT: Practical guide for radiologists. *Radiographics: A review publication of the Radiological Society of North America, Inc.* 2018; 38(2):450-61.
- Sonoda A, Nitta N, Ushio N, et al. Evaluation of the quality of CT images acquired with the single energy metal artifact reduction (SEMAR) algorithm in patients with hip and dental prostheses and aneurysm embolization coils. *Jpn. J. Radiol.* 2015; 33(11):710-6.
- Niu FY, Zhou Q, Yang JJ, et al. Distribution and prognosis of uncommon metastases from non-small cell lung cancer. *Bmc Cancer.* 2016; 16.
- Funama Y, Taguchi K, Utsunomiya D, et al. A newly-developed metal artifact reduction algorithm improves the visibility of oral cavity lesions on 320-MDCT volume scans. *Physica medica: PM: An international journal devoted to the applications of physics to medicine and biology: Official journal of the Italian Association of Biomedical Physics (AIFB).* 2015; 31(1):66-71.
- Yasaka K, Kamiya K, Irie R, et al. Metal artefact reduction for patients with metallic dental fillings in helical neck computed tomography: Comparison of adaptive iterative dose reduction 3D (AIDR 3D), forward-projected model-based iterative reconstruction solution (FIRST) and AIDR 3D with single-energy metal artefact reduction (SEMAR). *Dento maxillo facial radiology.* 2016; 45(7):20160114.
- Harnish R, Prevrhal S, Alavi A, et al. The effect of metal artefact reduction on CT-based attenuation correction for PET imaging in the vicinity of metallic hip implants: A phantom study. *Ann Nucl Med.* 2014; 28(6):540-50.
- Schabel C, Gatidis S, Bongers M, et al. Kupferschlaeger J, et al. Improving CT-Based PET Attenuation Correction in the Vicinity of Metal Implants by an Iterative Metal Artifact Reduction Algorithm of CT Data and Its Comparison to Dual-Energy-Based Strategies: A Phantom Study. *Invest. Radiol.* 2017; 52(1):61-5.
- van der Vos CS, Arens AIJ, Hamill JJ, et al. Metal Artifact Reduction of CT Scans to Improve PET/CT. *J Nucl Med.* 2017; 58(11):1867-72.

15. Kamel EM, Burger C, Buck A, et al. Impact of metallic dental implants on CT-based attenuation correction in a combined PET/CT scanner. *Eur Radiol.* 2003; 13(4):724-8.
16. Tateishi U, Tatsumi M, Terauchi T, et al. Relevance of monitoring metabolic reduction in patients with relapsed or refractory follicular and mantle cell lymphoma receiving bendamustine: A multicenter study. *Cancer Sci.* 2011; 102(2):414-8.
17. Kanda Y. Investigation of the freely available easy-to-use software 'EZR' for medical statistics. *Bone Marrow Transplant.* 2013; 48(3):452-8.
18. Chang Y, Xu D, Zamyatin AA, et al. Metal artifact reduction algorithm for single energy and dual energy CT scans. 2012 IEEE Nuclear Science Symposium and Medical Imaging Conference Record (NSS/MIC); 2012 27 Oct.-3 Nov. 2012.
19. Gondim Teixeira PA, Meyer JB, Baumann C, et al. Total hip prosthesis CT with single-energy projection-based metallic artifact reduction: Impact on the visualization of specific periprosthetic soft tissue structures. *Skeletal Radiol.* 2014; 43(9):1237-46.
20. Abdoli M, de Jong JR, Pruim J, et al. Reduction of artefacts caused by hip implants in CT-based attenuation-corrected PET images using 2-D interpolation of a virtual sinogram on an irregular grid. *Eur J Nucl Med Mol Imaging.* 2011; 38(12):2257-68.
21. Ay MR, Mehranian A, Abdoli M, et al. Qualitative and quantitative assessment of metal artifacts arising from implantable cardiac pacing devices in oncological PET/CT studies: A phantom study. *Mol Imaging Biol.* 2011; 13(6):1077-87.
22. Kennedy JA, Israel O, Frenkel A, et al. The reduction of artifacts due to metal hip implants in CT-attenuation corrected PET images from hybrid PET/CT scanners. *Med Biol Eng Comput.* 2007; 45(6):553-62.
23. Sher A, Lacoeyille F, Fosse P, et al. For avid glucose tumors, the SUV peak is the most reliable parameter for [(18)F]FDG-PET/CT quantification, regardless of acquisition time. *EJNMMI Res.* 2016; 6(1):21.